

Formation of mammalian pre-ribosomes proceeds from intermediate to composed state during ribosome maturation

Danysh A. Abetov^{1,6,π}, Vladimir S. Kiyan^{1,6,#}, Assylbek A. Zhylkibayev^{1,θ}, Dilara A. Sarbassova¹, Sanzhar D. Alybayev^{1,ω}, Eric Spooner², Min Sup Song^{1,3}, Rakhmetkazhy I. Bersimbaev⁴ and Dos D. Sarbassov^{1,3,5,*}

From the ¹Department of Molecular and Cellular Oncology, University of Texas MD Anderson Cancer Center, Houston, TX 77030; ²Whitehead Institute for Biomedical Research, Massachusetts Institute of Technology, Cambridge, MA 02142; ³The MD Anderson Cancer Center UTHealth Graduate School of Biomedical Sciences at Houston, TX 77030; ⁴Department of Natural Sciences, L.N. Gumilyov Eurasian National University, Nur-Sultan, Kazakhstan; ⁵Department of Biology, Nazarbayev University, Nur-Sultan, Kazakhstan

Running title: *Characterization of native mammalian pre-ribosomal complexes*

⁶Both authors contributed equally to this work.

Present addresses: ^πGraduate School, Cornell University, Ithaca NY 14853; [#]Head of the Research Platform of Agricultural Biotechnology, Department of Microbiology and Biotechnology, S. Seifullin Kazakh Agro Technical University, Nur-Sultan 010000 Kazakhstan; ^θSenior Research Scientist, Laboratory of Stem Cells, National Center for Biotechnology, Nur-Sultan 010000 Kazakhstan; ^ωGraduate School, Al-Farabi Kazakh National University, Almaty 050040 Kazakhstan

*To whom correspondence should be addressed: Dos D. Sarbassov, Department of Biology, Nazarbayev University, Nur-Sultan, Kazakhstan 010000; dos.sarbassov@nu.edu.kz; Tel. +7 (717)270-5873.

Keywords: ribosomal biogenesis, pre-ribosomal complexes, sucrose gradient fractionation, ribosomal biogenesis factors, ribosomal RNA processing, ribosomal RNA precursor, nutrient-dependent mTOR signaling, ribonucleoprotein (RNP) complex, composed pre-ribosome (CPRib), intermediate pre-ribosome (IPRib)

ABSTRACT

In eukaryotes, ribosome assembly is a rate-limiting step in ribosomal biogenesis that takes place in a distinctive sub-nuclear organelle, the nucleolus. How ribosomes get assembled at nucleolar site by forming initial pre-ribosomal complexes remains poorly characterized. In this study, using several human and murine cell lines, we developed a method for isolation of native mammalian pre-ribosomal complexes by lysing cell nuclei through mild sonication. A sucrose gradient fractionation of the nuclear lysate resolved several ribonucleoprotein (RNP) complexes containing rRNAs and ribosomal proteins. Characterization of the RNP complexes with MS-based protein identification and Northern blotting-based rRNA detection approaches identified two types of pre-ribosomes, we named here as intermediate pre-ribosomes (IPRibs) and composed pre-ribosome (CPRib). IPRib complexes comprised large pre-ribosomes (105S to 125S in size) containing the rRNA modification factors and pre-mature

rRNAs. We further observed that a distinctive CPRib complex consists of an 85S pre-ribosome assembled with mature rRNAs and a ribosomal biogenesis factor, Lyl antibody reactive (LYAR), that does not associate with pre-mature rRNAs and rRNA modification factors. rRNA-labeling experiments uncovered that IPRib assembly precedes formation of CPRib complex formation. We also found that formation of the pre-ribosomal complexes is nutrient dependent because the abundances of IPRib and CPRib decreased substantially when cells were either deprived of amino acids or exposed to an mTOR kinase inhibitor. These findings indicate that pre-ribosomes form via dynamic and nutrient-dependent processing events and progress from intermediate to composed state during ribosome maturation.

Introduction

Ribosomal biogenesis is a cellular biosynthetic process of constructing the massive ribonucleoprotein (RNP) complexes known as

ribosomes. It is an elaborate process that determines a rate of protein synthesis and, by controlling a main anabolic cellular process, it regulates accumulation of cellular mass or cell growth (1-3). An intensive and coordinated ribosomal biogenesis is crucial for eukaryotic cells because an evolutionary transition from prokaryotic to eukaryotic form of life is marked by a substantial increase in cell size. It is particularly relevant for mammalian cells considering that an average mammalian cell (15-20 μM diameter of cell) is at least 1000 times larger than a bacterial *E. coli* cell (1-1.5 μM diameter of cell) (4). In eukaryotes, a designated sub-nuclear organelle nucleolus has been evolved to accommodate an intensive ribosomal biogenesis (5-7). Nucleolus is a non-membrane bound organelle located in the nucleus and visualized as a dense particle at the chromatin sites of multiple ribosomal DNA (rDNA) repeats. Building of ribosomes is a main functional role of nucleoli where the massive ribosomal rDNA locus is integrated into a ribosomal construction site by various ribosomal biogenesis factors.

Ribosomal biogenesis is a dynamic process and it is determined by the rates of synthesis of ribosomal components including its rRNAs and multiple ribosomal proteins (79 in yeast or 80 in human cells), the active nuclear import of ribosomal proteins from cytoplasm to nucleus, the assembly of ribosomes and nuclear export of assembled ribosomes to cytoplasm (8,9). Assembly of ribosomes is a most elaborate and rate-limiting step in ribosomal biogenesis. Mature human 80 Svedberg (80S) ribosome is composed of two ribosomal subunits: a small 40S subunit representing the RNP complex of 18S rRNA and 33 distinct ribosomal proteins of small (RPS) subunit and a large 60S subunit is the RNP complex containing 28S, 5.8S and 5S rRNAs and 47 distinct ribosomal proteins of large (RPL) subunit. rRNAs make a core of both ribosomal subunits that prevail the ribosomal protein content by weight (10). Most of rRNAs are synthesized by the RNA polymerase I (Pol I) as a pre-cursor of rRNA (47S rRNA in mammalian cells, a transcript of 13 kb) at the nucleolar organizer regions (NORs) of nucleolus containing several hundred ribosomal DNA (rDNA) gene repeats residing in five clusters located on chromosomes 13, 14, 15, 21 and 22 of

human diploid cells. A newly synthesized rRNA precursor is processed rapidly by a proper folding and specific endonucleolytic cleavages coupled with exonuclease treatments to generate three rRNAs (18S, 5.8S and 28S) and Pol III synthesizes 5S rRNA by transcribing several hundred copies of 5S rDNA genes located on chromosome 1. Small nucleolar RNAs (snoRNAs) assembled into the conserved small nucleolar RNP (snoRNP) complexes also participate in rRNA processing by performing its specific covalent modifications (methylation, acetylation and pseudouridylation) that are critical for ribosomal assembly and function (8,9,11).

Assembly of both (40S and 60S) ribosomal subunits takes place simultaneously with the processing of rRNAs. According to the current model of eukaryotic ribosomal biogenesis, the rRNAs and ribosomal proteins get assembled at the granular zone of nucleolus by coalescing into a large 90S pre-ribosome. It is later divided into the pre-60S and pre-40S subunits that facilitates their exit from nucleus to cytoplasm through nuclear pores for their final maturation and functional localization (12). An enormous and delicate task of a simultaneous rRNA processing and assembly of ribosomes into 90S pre-ribosome is carried out by a large and highly diverse group of ribosomal biogenesis factors. The functional studies in yeast indicate that more than 350 nucleolar proteins (half of nucleolar proteins) participate in ribosomal biogenesis indicating a complexity of ribosomal assembly (7). Assembly of eukaryotic pre-ribosomes remains poorly characterized.

Eukaryotic native pre-ribosomal complexes and nascent rRNAs were detected in the original studies of 1970s (13,14). In 1975, a large RNP complex of 90S particle has been detected in the nuclear lysates of yeast by sucrose fractionation (14). Following this breakthrough finding, there were no active studies on characterization of pre-ribosomal complexes until the advances in proteomics. In 2002, Ed Hurt's laboratory has introduced and established a tandem affinity purification (TAP) method to purify pre-ribosomal complexes in yeast (15). The assumption was made that if a stably expressed recombinant protein was entering sucrose gradient and co-purified with ribosomal

RNAs, a recombinant protein is assembled into a pre-ribosomal complex. Based on this assumption, a TAP-purified complex has been isolated by expression of the ribosomal biogenesis factor Periodic Tryptophan Protein 2 (Pwp2 and also known as Utp1). The complex formed by a constitutively expressed Pwp2 did not show a sharp peak of 90S particle, but instead was dispersed across the sucrose gradient indicating a presence of heterogeneous complexes containing Pwp2 because of possible disintegration of a large complex. As the outcome of an initial assumption, the isolated Pwp2 complex by TAP-purification was named as 90S (15), not because of its actual size, but because of the original studies of 1970s (14). Thus, native pre-ribosomal complexes in eukaryotes have not been isolated and characterized and, for the last two decades, pre-ribosomal complexes at nucleolar site were studied by purification of the tagged recombinant proteins (7,16,17). A main purpose of the present study is to isolate and characterize mammalian pre-ribosomal complexes with a focus on optimizing nuclear lysis conditions to preserve native pre-ribosomal complexes and on carrying out their detection and characterization.

Results

Isolation of native mammalian pre-ribosomal complexes

Biochemical characterization of pre-ribosomal complexes is a challenging task because nucleoli are dense particles with heterogeneous segments (5,9,18). The fibrillar center (FC), dense fibrillar component (DFC) and granular component (GC) represent distinct segments of nucleoli known to carry out different functions. DFC or the border between DFC and FC regions is mostly assigned to the NOR areas for massive production of pre-rRNA carried out by Pol I transcription. While GC, a least dense segment of nucleoli, has been identified as a ribosomal assembly site. Considering that isolation of nucleoli requires a stringent lysis condition accompanied with sonication (19,20), it is possible that purification of nucleoli might cause disruption of GC and loss of pre-ribosomal complexes. To eliminate a potential loss of pre-ribosomal complexes in preparative steps of nucleolar enrichment, we chose to work with

isolated nuclei and optimize the nuclear lysis condition by an effective extraction of pre-ribosomal complexes without their disintegration (Supplementary Fig. 1).

We selected cancer cells for our studies because their accelerated growth is accommodated by intensive ribosomal biogenesis (18,21,22). As the primary step, we isolated intact nuclei from A549 cancer cells (a human adenocarcinoma lung cancer cell line) (23) and performed a stringent nuclear washing step to assure removal of mature cytoplasmic ribosomes and disruption of nuclear envelope. Purified nuclei were further lysed in the nuclear lysis buffer by a mild sonication to obtain the soluble nucleolar lysate that was further analyzed for presence of RNPs by a sucrose gradient fractionation. A mild sonication of nuclei was titrated to obtain optimal conditions to lyse nucleoli and release pre-ribosomal complexes without a substantial damage of pre-ribosomal complexes. We examined extraction of the nucleolar markers fibrillar and NOP56 (24,25) to monitor lysis of nucleoli. Obtained soluble nucleolar fraction was pre-cleared by centrifugation and the pre-cleared lysates were fractionated by ultracentrifugation on the linear 0%–50% sucrose gradient (Supplementary Fig. 2) with the parameters similar to resolve ribosomal particles and polysomes (26). A fractionation with continuous monitoring of RNA absorbance detected several RNP complexes resolved on the sucrose gradient (Fig. 1). We observed a sharp and high peak corresponding to a particle of 85S in size with RNA absorbance 1.1 ($A_{254}=1.1$). The other smaller peaks were corresponding to larger particles stretched from 125S to 105S. A largest particle among the trailing peaks was resolved as a 125S complex with RNA absorbance of 0.45 ($A_{254}=0.49$). We have characterized the resolved RNP complexes by analyzing their rRNA/protein compositions and rRNA labeling dynamics. According to our analysis, the sharp and high peak of 85S particle was detected in the fractions 17 and 18 and was named as the *Composed Pre-Ribosome (CPRib)* and the larger RNP particles stretching from fractions 21 to 26 were designated as the *Intermediate Pre-Ribosomes (IPRib)*. Partially overlapping peaks of IPRib complexes were further distinguished by size as the IPRib1 (125S

particles collected in the fractions 25 and 26), IPRib2 (115S particles collected in the fractions 23 and 24) and IPRib3 (105S particles collected in the fractions 21 and 22).

The similar (IPRib and CPRib) RNP complexes were detected by fractionation of the nuclear lysates obtained from human MDA-MB-231 (27), HCT116 (28), HeLa (29), mouse AK192 (30) cancer cells and mouse immortalized embryonic fibroblasts (MEFs) (31) shown in the Supplementary Figures 3 to 7. Analysis of the human primary lung MRC-5 and WI38 fibroblasts (32,33) also detected CPRib and IPRib complexes in their nuclear lysates (Supplementary Figs. 8 and 9).

The CPRib and IPRib complexes are distinguished not only by size but also by ribosomal biogenesis factors

To characterize the detected RNP (IPRib and CPRib) complexes, we performed the mass spectrometry analysis of the isolated IPRib and CPRib complexes from A549 and MDA-MB-231 human cancer cells. We performed the polyethylene glycol (PEG) precipitation of CPRib and IPRib complexes that is commonly used for isolation of ribosomal complexes from sucrose fractions (10). Most of RNAs within the obtained nuclear lysate were not associated with large complexes and remained on a surface of the sucrose gradient above fraction 5. We selected fraction 8 as the control fraction because it did not show presence of RNA. According the mass spectrometry analysis, the control fraction contained mostly RNA polymerase components and also 26S proteasome regulatory subunits. Most of ribosomal proteins of the large (60S) and small (40S) ribosomal subunits were found in the IPRib and CPRib fractions. 73 and 71 ribosomal proteins were detected by mass spectrometry in the pre-ribosomal fractions of A549 cells and MDA-MB-231 cells (Supplementary Tables 1 and 2 respectively) out of 80 known ribosomal proteins (34). To validate the proteomic data, we examined a presence of ribosomal proteins in the sucrose gradient fractions. It indicated that both CPRib and IPRib complexes contain the large (rpL5 and rpL26) and small (rpS6 and rpS11) ribosomal subunit proteins that were resolved from fraction 17 to fraction 26 (Fig. 2). We also observed distinct fractions representing 40S

particle contained only rpS11 and rpS6 proteins, but not rpL5 or rpL26 indicating that a small pre-40S ribosomal particle has been resolved as a barely detectable peak from the fractions 11 to 14. Our analysis shows that the resolved RNP complexes representing IPRib and CPRib fractions contain most of the ribosomal proteins of large and small ribosomal subunits.

The proteomics analysis was also instrumental to identify the distinct ribosomal biogenesis factors associated with the pre-ribosomal complexes. The lists of identified ribosomal biogenesis factors are shown in Supplementary Tables 3 (A549 cells) and 4 (MDA-MB-231 cells). We found that EBP2, Lasil and Brx1 (35) were detected in both CPRib and IPRib complexes and the presence of EBP2 was further validated by immunoblotting (Fig. 2). A ribosomal biogenesis factor LYAR (known also as cell growth-regulating nucleolar protein) (36) has been selectively enriched in CPRib fractions (Fig. 2 and Supplementary Tables 3 and 4). Most importantly, the rRNA modification factors known to be critical for the assembly and function of ribosomes were found in the IPRib fractions. We detected methyltransferase fibrillar and its interacting proteins NOP56 and NOP58 (24,25) in the IPRib fractions. These proteins are the components of the snoRNP complex known to assemble C/D box and play a crucial role in rRNA methylation. We also found that this complex plays a critical role in assembly of pre-ribosomes because the knockdown by shRNA targeting its central component NOP56 resulted in a substantial suppression of CPRib and IPRib formations (Supplementary Fig. 10). Besides the methyltransferase complex, IPRib complexes were also containing the rRNA acetylation factor RNA cytidine acetyltransferase (NAT10) (37,38), the rRNA pseudouridylation factor dyskerin pseudouridine synthase 1 (DKC1) (39,40) and also pescadillo ribosomal biogenesis factor 1 (PES1) with its interacting proteins Bop1 (41) (Fig. 2 and Supplementary Tables 3 and 4). We also detected other factors known to participate in ribosome assembly including rRNA processing HEAT repeat-containing protein 1 (42), RRP5 homolog (43), MKI67 FHA domain-interacting nucleolar phosphoprotein (44), U3 small nucleolar RNA-associated protein (45) in the IPRib fractions (Supplementary Tables 3 and

4). According to protein abundance (the sequenced peptide numbers and immunoblotting analysis), we observed an enrichment of the rRNA modification factors in the fractions corresponding to a largest IPRib complex (IPRib1). It suggests that IPRib1 is a core intermediate pre-ribosome that has been processed to the smaller IPRib2 and IPRib3 complexes during its maturation or it is partially disintegrated during the biochemical isolation. Thus, the pre-ribosomal CPRib and IPRib complexes are distinct not only by size, but also by the content of ribosomal biogenesis factors. The proteomic distinction of IPRib and CPRib implies their different functional roles in ribosomal biogenesis.

IPRib contains rRNA pre-cursors and its assembly precedes formation of CPRib

rRNAs are the core components of ribosomal subunits and we characterized rRNAs in the pre-ribosomal IPRib and CPRib complexes. Following isolation of the pre-ribosomes by PEG precipitation, we isolated RNA from the pre-ribosomal fractions by Trizol reagent and carried out Northern blot analysis by using oligonucleotides as the probes (Supplementary Fig. 11) for detecting rRNAs as described previously for analysis of rRNA processing (46). The total, nuclear and cytoplasmic RNAs were resolved in parallel as internal controls for detecting the differences between rRNA and its pre-cursor forms. Probing RNA blots with the oligonucleotide probes specific for detection of mature rRNAs (28S, 18S, 5.8S and 5S) did not show substantial differences among RNAs obtained from the CPRib and IPRib complexes indicating a presence of rRNAs in the nuclear RNP complexes (Fig. 3b). Surprisingly, only 5S rRNA was less abundant in the cytoplasmic fraction suggesting its important role in processing and assembly of ribosomes but not in the process of translation as described in the previous studies (47,48).

To detect the rRNA pre-cursors in the IPRib and CPRib fractions, we probed the membranes with the internal transcribed spacer 1 and 2 (ITS1 and ITS2) probes (Fig. 3a) (46). As expected, we observed a strong hybridization of

both ITS probes with the total and nuclear but not cytoplasmic RNAs indicating a presence of the rRNA pre-cursors only in the nuclear but not cytoplasmic fraction. As detected by both ITS1 and ITS2 probes, the pre-cursor rRNAs (30S and 32S) were found also in the IPRib fractions. Remarkably, abundance of 30S and 32S rRNAs was decreased substantially in the CPRib fraction (Fig. 3b). It indicates that ITS pre-cursors are mostly present in the IPRib complexes. We detected less pre-cursor rRNAs in the nuclear compare to the total RNA fraction. It might be explained by a sensitivity of the pre-cursor rRNAs to degradation during lysis of cells and isolation of nuclei. In addition, we also probed the membranes with the 5'ETS probe to detect a nascent 47S rRNA (early pre-cursor) and it has been detected mostly in the total RNA fraction and only its degraded fragments were observed in the nuclear and IPRib fractions (Supplementary Fig. 12). Thus, the 30S and 32S rRNA pre-cursors were observed in IPRib and much less in CPRib complexes.

We also assessed the dynamics of rRNA processing within the IPRib1 and CPRib complexes by performing the pulse-chase metabolic labeling of RNA with [³H] uridine according the established method (49). The [³H] uridine was added to the cells for 30 min for pulse labeling and was replaced with the medium containing “cold” non-labeled uridine for the indicated chase time (30, 60, 90 or 120 minutes). Following the chase incubations, the pulse labeled cells were lysed for the sub-cellular fractionation and the obtained nuclear fractions were further analyzed by the sucrose gradient fractionation to obtain the IPRib1 (the fractions 25 and 26) and CPRib (fractions 17 and 18) complexes. The pulse-chase experiment revealed that the labeled RNAs were detected within 30 min of chase in IPRib1 complex (Fig. 4a) and it took 4 times longer (120 min) to detect the pulsed RNA in CPRib complex (Fig. 4b). The pulse-chase experiment identified a substantial difference in dynamics of the IPRib and CPRib assembly revealing that IPRib forms prior to the formation of CPRib in a process of pre-ribosomal maturation.

Formation of IPRib and CPRib is nutrient dependent

A nutrient dependent regulation of ribosomal biogenesis is mediated by mTORC1 kinase activity known to control the rates of ribosomal protein synthesis (22,50) and transcription of rDNA (51-54). To study if pre-ribosomal complexes are sensitive to nutrient deprivation, we studied A549 cancer cells incubated in the medium without amino acids for different time points. A substantial decrease of the pre-ribosomal IPRib (1.9 fold) and CPRib (2.2 fold) peaks compared to the control has been detected within 1 hour of amino acid depletion (Fig. 5). The pre-ribosomal complexes were continuing to decrease following the third hour of starvation and were at least 2.6 folds smaller for IPRib and 2.8 folds for CPRib complexes (Supplementary Fig. 13). Besides, inhibition of the mTOR kinase activity by treating A549 cancer cells with a potent mTOR kinase inhibitor Torin 1 for one hour mimicked the amino acid deprivation effect by causing a significant decrease in abundance of IPRib (2.8 fold) and CPRib (2.7 fold) (Fig. 6) that has been slightly recovered following the third hour of inhibition indicating only 2.3 fold decrease for both CPRib and IPRib complexes (Supplementary Fig. 14). These findings show that the amino acid impact was increasing from 1 to 3 hour of the nutrient deprivation, whereas the drug effect was stronger at its first hour and its effect was gradually decreasing following a third hour of treatment. Thus, we show that inhibition of the nutrient-dependent mTORC1 signaling known to control ribosomal biogenesis leads to suppression of the pre-ribosomal assembly as detected by low peaks of IPRib and CPRib complexes.

This study shows that CPRib presented as an 85S particle is distinct from a cytoplasmic 80S ribosome. It is well known that abundance of 80S ribosomes increases substantially following inhibition of the nutrient-dependent mTORC1 signaling because disintegration of polysomes leads to the accumulation of ribosomal 80S particles (55,56). We examined the cytoplasmic fractions isolated from actively growing A549 cancer cells or cells treated with Torin 1 (55). The sucrose fractionation study indicated six-fold increase of the cytoplasmic 80S peak following inhibition of mTORC1 by Torin 1 for three hours (Supplementary Fig. 15). Inhibition of the

mTORC1 signaling by Torin 1 was validated by analysis of S6K1 phosphorylation according to our previous studies (57,58). Besides, the CPRib and IPRib pre-ribosomal complexes did not show presence of the endoplasmic reticulum (ER, [ER57 or eIF2 α]) and mitochondria (ATP synthase β) proteins (Supplementary Fig. 16) that is coherent with a nuclear assembly of the identified pre-ribosomes. Detection of the nucleolar markers fibrillarin, BOP1 and DDX18 (7,24, 25,41) in the pre-ribosomal fractions but not in the cytoplasmic fraction (Supplementary Fig. 16) has further validated the fractionation method and protein detection analysis by mass spectrometry (Supplementary Tables 3 and 4).

Thus, our study indicates CPRib and 80S ribosomes behave opposite in response to mTOR inhibition indicating that they represent different RNP complexes although similar in size.

Discussion

A dense nucleolar structure is the main problem in isolation of eukaryotic pre-ribosomal complexes. The problem has been circumvented by introduction of a recombinant protein purification method (15). It became the main approach in isolation of pre-ribosomal complexes by an effective affinity purification method of tagged proteins since 2002. The isolation of native eukaryotic pre-ribosomal complexes has not been actively pursued since 1975 (14). In our study, we isolated and characterized the mammalian native pre-ribosomal complexes that were named as IPRib and CPRib complexes. We developed a method of mammalian pre-ribosomes isolation by performing mild sonication of nuclei and detecting pre-ribosomal RNP complexes by fractionation in a sucrose gradient. To prevent co-purification of residual cytoplasmic ER or mitochondrial ribosomes with intact nuclei, prior to the sonication step, the nuclei were incubated in a stringent buffer. A mild sonication of nuclei became a critical step in obtaining the pre-ribosomal complexes and this step that has been optimized in order to balance an extraction and preservation of the IPRib and CPRib complexes. We found that a sucrose gradient fractionation developed for profiling of ribosomes and polysomes is also optimal for profiling of the pre-ribosomal complexes by fractionation of the nuclear lysates. The

fractionation has been optimized to preserve integrity of the pre-ribosomal complexes by introducing a linear sucrose gradient from 0% to 45% with a slow acceleration mode of ultracentrifuge runs. The isolation of pre-ribosomal complexes has been validated in a wide range of mammalian (human and mouse) cells including cancer and primary cell lines.

We show that the mild sonication of nuclei is sufficient to extract two distinct pre-ribosomal complexes representing the intermediate and assembled (composed) stages of their formation. Detected large IPRib complexes were defined as the intermediate pre-ribosomes because they contain pre-mature rRNA (30S and 32S) (46) and rRNA modification factors (fibrillarin, Nat10 and DKC1) (11). Considering its RNA/protein composition and dynamics of assembly, IPRibs represent a ribosomal assembly stage at which rRNAs get methylated, acetylated or pseudouridinylated on specific sites required for proper ribosomal assembly and function (1,11,37). This finding indicates that the rRNA modification factors form a large complex with a pre-ribosome to carry out the modifications of rRNAs. The rRNA modification factors might exist as a multi-functional platform that forms a transitional complex with pre-ribosome to perform different types of rRNA modifications simultaneously and with high fidelity. While an existence of the rRNA modification platform is yet to be defined, our study shows that IPRibs are transitional and intermediate pre-ribosome associated with the rRNA modification factors. A transitional state of IPRib might explain why they are unstable complexes, which are much more sensitive to the lysis conditions compared to CPRib. We find that prolongation of the sonication step resulted in a much less of IPRib but increased extraction of CPRib. It is also possible that the largest intermediate pre-ribosome IPRib1 (a 125S particle) is the main complex that is disintegrated to the smaller IPRib2 (115S) and IPRib3 (105S) pre-ribosomal particles in a process of sonication. Detection of labeled rRNA within 30 min time point of chase indicates a rapid assembly of IPRib that is coherent with the dynamics of rRNA modification. A presence of rRNA modification factors is the distinctive feature of IPRib complexes that suggests their functional role in

mediating specific rRNA modifications known to be critical for rRNA processing in ribosomal biogenesis (11).

According to our study CPRib is an abundant native mammalian 85S pre-ribosome. Considering resemblance of CPRib by size to the yeast 90S pre-ribosomal particle observed in the original study of 1975 (14), we interpret that CPRib is most likely a native eukaryotic 90S pre-ribosome. To avoid confusion with 90S pre-ribosome purified by expression of the recombinant PWP2 protein, we named the abundant 85S RNP complex as CPRib to reflect a composed (assembled and tranquil) state of a mammalian pre-ribosome. Characterization of CPRib has distinguished it from larger IPRib complexes by its composition, assembly dynamics and stability. In contrary to IPRib, CPRib contains only mature rRNAs and a ribosomal biogenesis factor LYAR that is marked by the absence of rRNA modification factors. The pulse-chase RNA labeling study indicated that CPRib is formed at the final stage of ribosomal biogenesis that corresponds with the dynamics of mammalian ribosome formation. A stable nature of CPRib also reflects an assembled state of pre-ribosome, which remains intact even following a consecutive second sucrose fractionation (data not shown). Our study indicates that CPRib presents an assembled pre-ribosome that is formed following completion of an intermediate phase of rRNA processing. A functional relevance of CPRib is yet to be determined, but it is likely an assembled pre-ribosomal state in transition to become a functional ribosome where LYAR holds it at a locked non-translate conformation prior to its export from the nucleus to cytoplasm mediated by dissociation of the pre-ribosome in two pre-40S and pre-60S subunits.

Ribosomal assembly at the nucleolar site remains poorly characterized. Characterization of pre-ribosomal complexes will be instrumental to determine how ribosomal assembly and processing take place at nucleolar site. We show that mild sonication of nuclei obtained from mammalian cells is an effective approach to extract and isolate the intermediate and composed (late or assembled) pre-ribosomal complexes. It is likely that early pre-ribosomes with nascent rRNAs (47S-45S) are fragile complexes sensitive to mild sonication and development of more

delicate extraction conditions will be necessary to isolate early pre-ribosomes. Abundance of pre-ribosomal complexes is tightly regulated and nutrient deprivation or inhibition of mTOR at least for 1 hour is sufficient to decrease the pre-ribosomal RNP peaks. Dynamics of a nutrient-dependent impact on the pre-ribosomal complexes indicates that a nutrient-dependent mTOR signaling coordinates assembly of pre-ribosomal complexes and functional activities of the ribosomal biogenesis factors. How the nutrient-sensitive mTORC1 complex residing in cytoplasm regulates assembly of pre-ribosomes at the nucleolar site is yet to be determined. The mechanism could be related to mTOR-dependent regulation of rDNA transcription by RNA Polymerase I (51-54) that also remains to be characterized.

Experimental procedures

Cell culture and cell lines

The human A549, MDA-MB-231, HCT116, WI38 and MRC5 cell lines were obtained from the American Type Cell Culture Collection (ATCC) and the mouse AK192 cancer cells were described previously(30). Cells cultured at 37°C in a humidified incubator were maintained in the DMEM/Ham'sF12 medium (catalog #DFL13 from Caisson Labs) and supplemented with 10% FCS, 2 mM glutamine and penicillin (100 units/ml)-streptomycin (100 µg/ml). Five million of A549 cancer cells were cultured on 145 mm dishes in 20 ml of cell culture medium and were growing for 48 hrs (reaching approximately 14 million cells) to perform the sub-cellular fractionation and obtain the nuclear or cytoplasmic fractions. Other cell lines were split to 50% density into 145 mm dishes in 20 ml of cell culture medium and were growing for 48 hours prior to the sub-cellular fractionation. About 4-6 plates of cancer cells or 12 plates of primary cells were lysed to obtain the nuclear fraction for one gradient fractionation. The knockdown of NOP56 in A549 cells was performed by lentiviral expression of shRNA targeting luciferase (control) or NOP56 (obtained from Sigma-Aldrich, Clone ID: NM_006392.2-462s21c1 with the following sequence CCGGACCGATCTGTC

AGCTTGTAAGCTCGAGTTTACAAGCTGGATCGGTTTTTTG) according to our previous study (31).

Sub-cellular fractionation to obtain the soluble nuclear fractions from mammalian cells

All steps of the sub-cellular fractionation were performed in cold at 4° C. Cells with or without treatment were washed twice with 15 ml ice cold PBS. To aspirate most of PBS, the plates were kept at vertical position for at least 30 seconds. Washed cells were lysed in 0.6 ml Magnesium (Mg) Buffer per plate. Mg buffer composition: 40 mM Hepes-NaOH pH-7.5, 160 mM KCl, 10 mM MgCl₂, 0.5% Glycerol, 0.5% NP40. The prepared Mg buffer stock was kept frozen at -20° C, the defrosted aliquots were kept at 4° C and used within one month. Prior to use, Mg buffer was supplemented with the Phosphatase Inhibitors (Biotool) and Protease Inhibitor (Roche) according the manufactures' instructions. Lysates from two plates were collected by scraping into 2 ml tube and were incubated for 30 min by rotation in cold room. After incubation, the lysates were spun at x500 g for 5 min to obtain the cytoplasm (supernatant) and nuclei (pellet). Nuclei were washed in 1 ml of Mg Buffer without detergent and resuspended by flicking and rotating the tube 5-6 times followed by an additional spin at x500 g for 5 min to obtain the nuclei by discard the supernatant. The nuclei were further washed under stringent conditions by adding 0.4 ml of Nuclear Lysis buffer described below (with MgCl₂ but without the protease and phosphates inhibitors) and incubating by gentle rotations for 15 min in the cold room. The stringent washing step has been introduced to remove any residual cytoplasmic components including mitochondria and to perforate the nuclear envelope. After the stringent wash, nuclei were collected by spinning at x500 g for 5 min and washed again with 1 ml of Mg Buffer without detergent by flicking and rotating the tube 5-6 times. After the final wash, the nuclei from 4 plates (145 mm cell culture plates) were collected in one tube by spinning at x500 g for 5 min.

Sucrose gradient fractionation

The pellets of nuclei obtained from 4 plates (145 mm cell culture plates) and combined in one 1.5 ml tube were lysed in 0.4 ml of Nuclear Lysis

buffer (NLB): 10 mM Tris HCl, pH 8.0, 2.5mM MgCl₂, 1.5 mM KCl, 0.5% Triton X100, 0.5% Deoxycholate (NLB stock has been prepared without MgCl₂, aliquoted and kept frozen at minus 20° C, prior to use the buffer aliquote was defrosted and supplemented with MgCl₂ and also Phosphatase Inhibitors [Biotool] and Protease Inhibitor [Roche] according the manufactures' instructions). To perform a mild nuclear lysis, nuclei were resuspended by brief pipetting and sonicated by Bioruptor (Diagenode) for 4 cycles at the low-level setting. Each cycle was carried out for 15 seconds of sonication and 30 seconds of pausing. For effective nuclear lysis, the final volume should not exceed 0.6 ml. Following sonication step, the soluble nuclear fraction (NSF) was obtained by spinning the nuclear lysates for 15 min at 20,000xg at 4° C. About 1.5 mg of NSF was loaded on the top of a linear sucrose gradient tube (0%-50%). The sucrose gradients were made in the sucrose gradient buffer (20 mM Hepes pH-7.5, 100 mM KCl and 5 mM MgCl₂) by adding equal volume of 50% sucrose to the bottom of a tube containing 0% sucrose to the ultracentrifugation tubes (Seton, cat#7030). The BioComp Gradient station with Triax Flow Cell 1 (FC-1) from BioComp Instruments (Fredericton, Canada) was instrumental to obtain the highly reproducible linear sucrose gradients and perform the automated fractionation analysis (59,60). The linear sucrose gradients were prepared by the BioComp Gradient station with optimized eleven-step gradient making program described in Supplementary Figure 2. The NSF samples were fractionated by ultracentrifugation for 3h 45 min at 35,000xg at 4° C by running Beckman Optima ultracentrifuge with SW41 Ti swinging bucket rotor with the setting for acceleration 9 and deceleration 4. Following ultracentrifugation, the sucrose gradients were fractionated by the BioComp Gradient station with Triax FC-1 for monitoring of ultraviolet light (254 nm wavelength) absorbance for detection of pre-ribosomal RNP complexes by obtaining 28 fractions. Initially, detection of pre-ribosomal RNP complexes was carried out by using the BioComp Gradient station with Bio-Rad EM1 that proceeded by mechanical navigation of fractionation and collecting 26 fractions (Supplementary Figs. 4-6 and 10).

Isolation of the pre-ribosomal complexes

Sedimentation coefficients of the IPRib and CPRib pre-ribosomal complexes were calculated relative to sedimentation of the known cytoplasmic ribosomal particles. Detected RNP complexes in the sucrose fractions were isolated by PEG precipitation or analyzed by boiling the sucrose fraction aliquots with protein loading buffer for the immunoblotting analysis. The fractions containing the RNP complexes were combined for polyethylene glycol (PEG) precipitation (10). PEG 20000 was added to reach 7% of its final concentration, KCl was adjusted to 350 mM, MgCl₂ to 5 mM and Tris HCl pH-7.5 to 20 mM. Following mixing, the tubes were incubated on ice for 30 min. After the incubation, the tubes were centrifuged at 17,400xg for 15 min at 4° C and supernatant was removed by leaving approximately 100-150 µl of the solution. The samples were centrifuged again at 14,000xg for 5 min to remove residual PEG 20000 solution. Precipitated RNP complexes were further studied by isolating RNA with Trizol reagent according manufacture's instructions or boiling in the protein loading buffer.

Protein identification by mass spectrometry

Following resolving of denatured proteins in 10% polyacrylamide gel by a short run (20 min), the gel was stained by GelCode Blue Stain Reagent (#24590, Thermo Scientific) overnight and washed in water for 2 hours. Stained protein lanes were excised, reduced, alkylated and digested with trypsin at 37° C overnight. The resulting peptides were extracted, concentrated and injected onto a Waters NanoAcquity HPLC equipped with a self-packed Aeris 3 µm C18 analytical column (0.075 mm by 20 cm, Phenomenex). Peptides were eluted using standard reverse-phase gradients. The effluent from the column was analyzed using a Thermo Orbitrap Elite mass spectrometer (nanospray configuration) operated in a data dependent manner. The resulting fragmentation spectra were correlated against the known database using Mascot (Matrix Science). Scaffold Q+S (Proteome Software) was used to provide consensus reports for the identified proteins.

rRNA detection by Northern blot

RNA isolated from pre-ribosomal complexes, cells or sub-cellular fractions were resolved in 1% agarose gel containing 7% formaldehyde in 1XTT buffer (30 mM Tricine and 30 mM Triethanolamine). The RNA samples were loaded on a gel by mixing with a same volume of 2XRNA loading dye (NEB, cat#B0363A) and incubated at 85° C for 2 min. Resolved RNAs were transferred to the nylon membrane (Amersham Hybond-XL, GE Healthcare, Cat#RPN203S) overnight by capillary downward absorption of 10X SSC buffer using a stack of Kimberly-Clark WypAll papers (61). Following the transfer, nylon membranes were baked at 80° C for 30 min to achieve irreversible binding of RNA to the membranes. Membranes were pre-hybridized and hybridized in Perfecthyb plus Buffer (Sigma, cat#H7033) by incubation with a continuous rotation. Specific oligonucleotides were end-labeled with [γ -32P] ATP and T4 polynucleotide kinase (New England Biolabs #M0201S) according the manufacture's protocol and used as the probes following isolation of labeled oligonucleotides by Mini Quick Spin DNA columns (Roche #11814419001). Membranes pre-hybridized at 55° C for 1 hour were hybridized with the oligonucleotide probes dissolved in Perfecthyb plus Buffer (1-1.5x10⁶ CPM/ml) by incubation at 55 or 60° C overnight. Sequences of the probes complementary to different areas of 47S rRNA are shown in Supplementary Figure 11. Following hybridization, the membranes were washed at 55° C and exposed to X-ray films.

RNA labeling and detection of incorporated [5,6-³H] uridine

RNA labeling was performed according the previous study (49). For the pulse labeling, [5,6-³H] uridine (Perkin Elmer #NET367001MC) was added to the medium of actively growing A549 cells to a final concentration of 3 μ Ci/ml for 30

min. The labeled uridine was replaced with cold (1 mM) uridine for the indicated chase time. Following pulse/chase labeling, the cells were lysed to obtain the pre-ribosomal complexes as described above and the pre-ribosomal RNAs resolved on a gel and transferred to membrane were analyzed by autoradiography enhancement to detect incorporated [5,6-³H] uridine. For autoradiography enhancement, baked nylon membranes were incubated in methyl anthranilate containing 0.5% 2,5-diphenyloxazole for 5 min at room temperature according the original study (62). Membranes were dried for five minutes on tissue napkins and exposed to X-Ray film at -80° C overnight or 2-3 days.

Immunoblotting

For protein detection, the sucrose gradient fractions or cellular lysates were boiled by adding a same volume of 2X protein loading buffer or pre-ribosomal complexes enriched by PEG 20000 precipitation were boiled in 1X protein loading for 5 min. After boiling the protein samples were resolved in 4%-15% gradient gels (mini or midi gels from Bio-Rad) and transferred to polyvinylidene difluoride (PVDF) membrane by electrophoresis. The proteins were then visualized by immunoblotting with specific antibodies and detected with chemiluminescence Clarity™ Western ECL Substrate (Bio-Rad, cat# 170-5061). The antibodies against ribosomal proteins and nucleolar proteins used in this study were obtained from Bethyl (Montgomery, TX). The antibodies against ATP synthase β antibody (#A21351 from Thermo Fisher Scientific, Waltham, MA), ER57 (#05-728 from EMD Millipore, Billerica, MA) and eIF2 α (#9722, Cell Signaling Technology, Danvers, MA) were used for detecting the ER and mitochondrial markers.

Acknowledgements:

We thank Dr. David Coomb (Fredericton, Canada) for developing Triax Flow Cell system. It advanced the gradient fractionation to a fully automated process and was instrumental for detection and isolation of pre-ribosomal complexes in our study. We also grateful to our departmental colleague Dr. Haoqiang Ying for providing the mouse AK192 cancer cell line.

Conflict of interest: The authors declare that they have no conflicts of interest with the contents of this article.

Author contributions:

D.D.S. conceived the project, analyzed data and designed experiments. D.A.A. performed the studies of isolation and analyzing the pre-ribosomal complexes, V.S.K. developed the method of pre-ribosomal isolation by introducing nuclear sonication. A.A.Z., D.A.S. and S.D.A optimized the method and performed pre-ribosomal analysis on the different cancer and primary cell lines. D.A.S. and D.D.S. wrote the manuscript. E.S. performed the proteomics analysis, M.S.S and R.I.B. analyzed and interpreted data.

References

1. Nazar, R. N. (2004) Ribosomal RNA processing and ribosome biogenesis in eukaryotes. *IUBMB life* **56**, 457-465
2. Thomson, E., Ferreira-Cerca, S., and Hurt, E. (2013) Eukaryotic ribosome biogenesis at a glance. *Journal of cell science* **126**, 4815-4821
3. Lempiainen, H., and Shore, D. (2009) Growth control and ribosome biogenesis. *Current opinion in cell biology* **21**, 855-863
4. Moran, U., Phillips, R., and Milo, R. (2010) SnapShot: key numbers in biology. *Cell* **141**, 1262-1262 e1261
5. Lam, Y. W., Trinkle-Mulcahy, L., and Lamond, A. I. (2005) The nucleolus. *Journal of cell science* **118**, 1335-1337
6. Pederson, T. (2011) The nucleolus. *Cold Spring Harbor perspectives in biology* **3**
7. Klinge, S., and Woolford, J. L., Jr. (2018) Ribosome assembly coming into focus. *Nature reviews. Molecular cell biology*
8. Nerurkar, P., Altvater, M., Gerhardy, S., Schutz, S., Fischer, U., Weirich, C., and Panse, V. G. (2015) Eukaryotic Ribosome Assembly and Nuclear Export. *International review of cell and molecular biology* **319**, 107-140
9. de la Cruz, J., Karbstein, K., and Woolford, J. L., Jr. (2015) Functions of ribosomal proteins in assembly of eukaryotic ribosomes in vivo. *Annual review of biochemistry* **84**, 93-129
10. Yusupova, G., and Yusupov, M. (2014) High-resolution structure of the eukaryotic 80S ribosome. *Annual review of biochemistry* **83**, 467-486
11. Watkins, N. J., and Bohnsack, M. T. (2012) The box C/D and H/ACA snoRNPs: key players in the modification, processing and the dynamic folding of ribosomal RNA. *Wiley interdisciplinary reviews. RNA* **3**, 397-414
12. Tschochner, H., and Hurt, E. (2003) Pre-ribosomes on the road from the nucleolus to the cytoplasm. *Trends in cell biology* **13**, 255-263
13. Warner, J. R., and Soeiro, R. (1967) Nascent ribosomes from HeLa cells. *Proceedings of the National Academy of Sciences of the United States of America* **58**, 1984-1990
14. Trapman, J., Retel, J., and Planta, R. J. (1975) Ribosomal precursor particles from yeast. *Experimental cell research* **90**, 95-104
15. Grandi, P., Rybin, V., Bassler, J., Petfalski, E., Strauss, D., Marzioch, M., Schafer, T., Kuster, B., Tschochner, H., Tollervey, D., Gavin, A. C., and Hurt, E. (2002) 90S pre-ribosomes include the 35S pre-rRNA, the U3 snoRNP, and 40S subunit processing factors but predominantly lack 60S synthesis factors. *Molecular cell* **10**, 105-115
16. Kornprobst, M., Turk, M., Kellner, N., Cheng, J., Flemming, D., Kos-Braun, I., Kos, M., Thoms, M., Berninghausen, O., Beckmann, R., and Hurt, E. (2016) Architecture of the 90S Pre-ribosome: A Structural View on the Birth of the Eukaryotic Ribosome. *Cell* **166**, 380-393
17. Sun, Q., Zhu, X., Qi, J., An, W., Lan, P., Tan, D., Chen, R., Wang, B., Zheng, S., Zhang, C., Chen, X., Zhang, W., Chen, J., Dong, M. Q., and Ye, K. (2017) Molecular architecture of the 90S small subunit pre-ribosome. *eLife* **6**
18. Derenzini, M., Trere, D., Pession, A., Montanaro, L., Sirri, V., and Ochs, R. L. (1998) Nucleolar function and size in cancer cells. *The American journal of pathology* **152**, 1291-1297
19. Andersen, J. S., Lam, Y. W., Leung, A. K., Ong, S. E., Lyon, C. E., Lamond, A. I., and Mann, M. (2005) Nucleolar proteome dynamics. *Nature* **433**, 77-83
20. Li, Z. F., and Lam, Y. W. (2015) A new rapid method for isolating nucleoli. *Methods Mol Biol* **1228**, 35-42
21. Guertin, D. A., and Sabatini, D. M. (2005) An expanding role for mTOR in cancer. *Trends in molecular medicine* **11**, 353-361
22. Guertin, D. A., and Sabatini, D. M. (2007) Defining the role of mTOR in cancer. *Cancer cell* **12**, 9-22
23. Giard, D. J., Aaronson, S. A., Todaro, G. J., Arnstein, P., Kersey, J. H., Dosik, H., and Parks, W. P. (1973) In vitro cultivation of human tumors: establishment of cell lines derived from a series of solid tumors. *Journal of the National Cancer Institute* **51**, 1417-1423

24. Hayano, T., Yanagida, M., Yamauchi, Y., Shinkawa, T., Isobe, T., and Takahashi, N. (2003) Proteomic analysis of human Nop56p-associated pre-ribosomal ribonucleoprotein complexes. Possible link between Nop56p and the nucleolar protein treacle responsible for Treacher Collins syndrome. *The Journal of biological chemistry* **278**, 34309-34319
25. Lechertier, T., Grob, A., Hernandez-Verdun, D., and Roussel, P. (2009) Fibrillarin and Nop56 interact before being co-assembled in box C/D snoRNPs. *Experimental cell research* **315**, 928-942
26. Gandin, V., Sikstrom, K., Alain, T., Morita, M., McLaughlan, S., Larsson, O., and Topisirovic, I. (2014) Polysome fractionation and analysis of mammalian translomes on a genome-wide scale. *Journal of visualized experiments : JoVE*
27. Kapoor, C. L., and Cho-Chung, Y. S. (1983) Mitotic apparatus and nucleoli compartmentalization of 50,000-dalton type II regulatory subunit of cAMP-dependent protein kinase in estrogen receptor negative MDA-MB-231 human breast cancer cells. *Cell biology international reports* **7**, 49-60
28. Deschoolmeester, V., Boeckx, C., Baay, M., Weyler, J., Wuyts, W., Van Marck, E., Peeters, M., Lardon, F., and Vermorken, J. B. (2010) KRAS mutation detection and prognostic potential in sporadic colorectal cancer using high-resolution melting analysis. *British journal of cancer* **103**, 1627-1636
29. Landry, J. J., Pyl, P. T., Rausch, T., Zichner, T., Tekkedil, M. M., Stutz, A. M., Jauch, A., Aiyar, R. S., Pau, G., Delhomme, N., Gagneur, J., Korbel, J. O., Huber, W., and Steinmetz, L. M. (2013) The genomic and transcriptomic landscape of a HeLa cell line. *G3 (Bethesda)* **3**, 1213-1224
30. Ying, H., Kimmelman, A. C., Lyssiotis, C. A., Hua, S., Chu, G. C., Fletcher-Sananikone, E., Locasale, J. W., Son, J., Zhang, H., Coloff, J. L., Yan, H., Wang, W., Chen, S., Viale, A., Zheng, H., Paik, J. H., Lim, C., Guimaraes, A. R., Martin, E. S., Chang, J., Hezel, A. F., Perry, S. R., Hu, J., Gan, B., Xiao, Y., Asara, J. M., Weissleder, R., Wang, Y. A., Chin, L., Cantley, L. C., and DePinho, R. A. (2012) Oncogenic Kras maintains pancreatic tumors through regulation of anabolic glucose metabolism. *Cell* **149**, 656-670
31. Chen, C. H., Shaikenov, T., Peterson, T. R., Aimbetov, R., Bissenbaev, A. K., Lee, S. W., Wu, J., Lin, H. K., and Sarbassov dos, D. (2011) ER stress inhibits mTORC2 and Akt signaling through GSK-3beta-mediated phosphorylation of rictor. *Sci Signal* **4**, ra10
32. Yamamoto, R., Lin, L. S., Lowe, R., Warren, M. K., and White, T. J. (1990) The human lung fibroblast cell line, MRC-5, produces multiple factors involved with megakaryocytopoiesis. *J Immunol* **144**, 1808-1816
33. McSwiggan, D. A., Darougar, S., Rahman, A. F., and Gibson, J. A. (1975) Comparison of the sensitivity of human embryo kidney cells, HeLa cells, and WI38 cells for the primary isolation of viruses from the eye. *Journal of clinical pathology* **28**, 410-413
34. Ishii, K., Washio, T., Uechi, T., Yoshihama, M., Kenmochi, N., and Tomita, M. (2006) Characteristics and clustering of human ribosomal protein genes. *BMC genomics* **7**, 37
35. Shimoji, K., Jakovljevic, J., Tsuchihashi, K., Umeki, Y., Wan, K., Kawasaki, S., Talkish, J., Woolford, J. L., Jr., and Mizuta, K. (2012) Ebp2 and Brx1 function cooperatively in 60S ribosomal subunit assembly in *Saccharomyces cerevisiae*. *Nucleic acids research* **40**, 4574-4588
36. Miyazawa, N., Yoshikawa, H., Magae, S., Ishikawa, H., Izumikawa, K., Terukina, G., Suzuki, A., Nakamura-Fujiyama, S., Miura, Y., Hayano, T., Komatsu, W., Isobe, T., and Takahashi, N. (2014) Human cell growth regulator Ly-1 antibody reactive homologue accelerates processing of preribosomal RNA. *Genes to cells : devoted to molecular & cellular mechanisms* **19**, 273-286
37. Ito, S., Horikawa, S., Suzuki, T., Kawauchi, H., Tanaka, Y., Suzuki, T., and Suzuki, T. (2014) Human NAT10 is an ATP-dependent RNA acetyltransferase responsible for N4-acetylcytidine formation in 18 S ribosomal RNA (rRNA). *The Journal of biological chemistry* **289**, 35724-35730
38. Sharma, S., Langhendries, J. L., Watzinger, P., Kotter, P., Entian, K. D., and Lafontaine, D. L. (2015) Yeast Kre33 and human NAT10 are conserved 18S rRNA cytosine acetyltransferases that modify tRNAs assisted by the adaptor Tan1/THUMP1. *Nucleic acids research* **43**, 2242-2258
39. Jack, K., Bellodi, C., Landry, D. M., Niederer, R. O., Meskauskas, A., Musalgaonkar, S., Kopmar, N., Krasnykh, O., Dean, A. M., Thompson, S. R., Ruggero, D., and Dinman, J. D. (2011) rRNA pseudouridylation defects affect ribosomal ligand binding and translational fidelity from yeast to human cells. *Molecular cell* **44**, 660-666

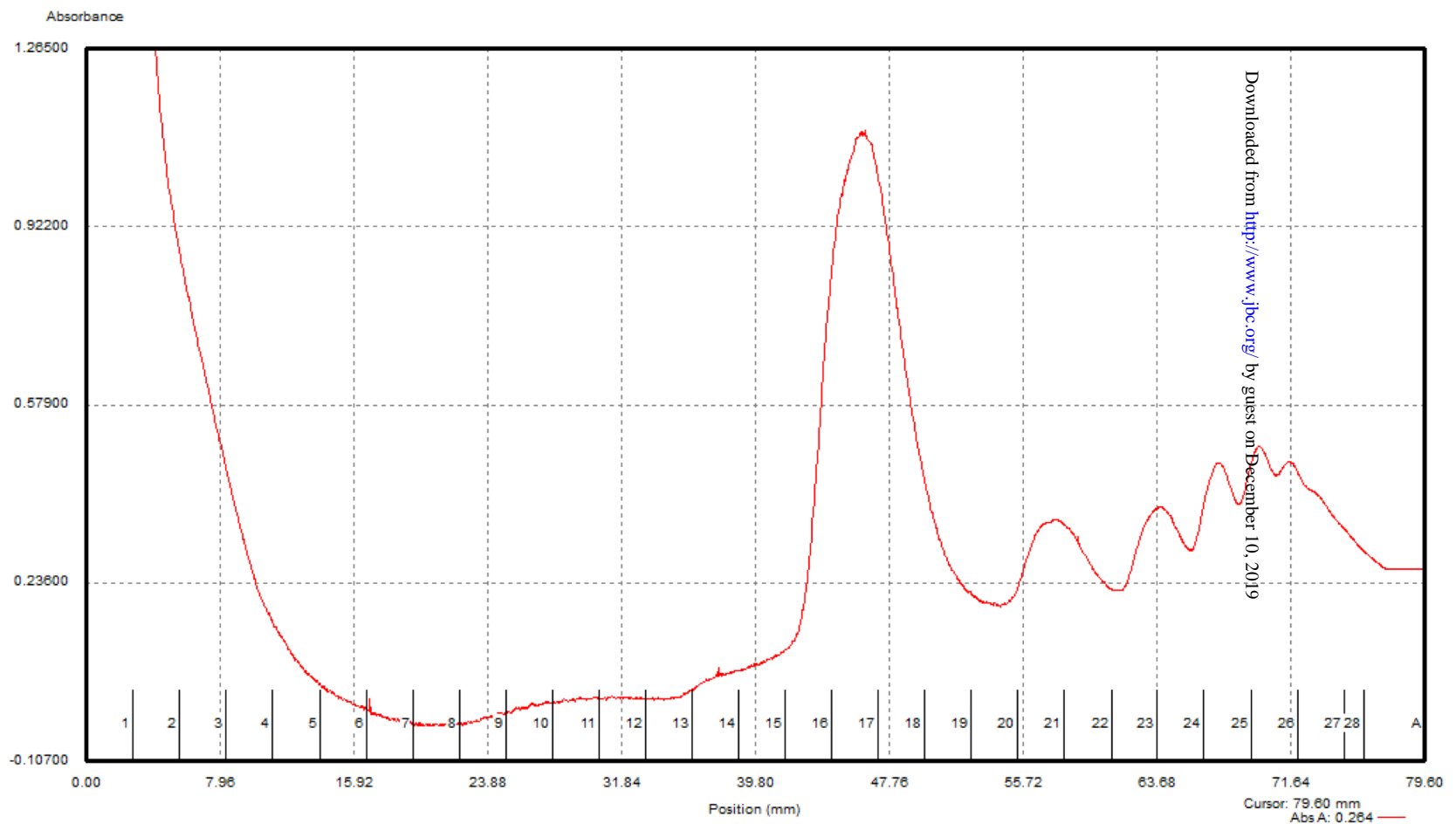
40. Ruggero, D., Grisendi, S., Piazza, F., Rego, E., Mari, F., Rao, P. H., Cordon-Cardo, C., and Pandolfi, P. P. (2003) Dyskeratosis congenita and cancer in mice deficient in ribosomal RNA modification. *Science* **299**, 259-262
41. Holzel, M., Rohmoser, M., Schlee, M., Grimm, T., Harasim, T., Malamoussi, A., Gruber-Eber, A., Kremmer, E., Hiddemann, W., Bornkamm, G. W., and Eick, D. (2005) Mammalian WDR12 is a novel member of the Pes1-Bop1 complex and is required for ribosome biogenesis and cell proliferation. *The Journal of cell biology* **170**, 367-378
42. Dez, C., Dlakic, M., and Tollervey, D. (2007) Roles of the HEAT repeat proteins Utp10 and Utp20 in 40S ribosome maturation. *RNA* **13**, 1516-1527
43. Turner, A. J., Knox, A. A., Prieto, J. L., McStay, B., and Watkins, N. J. (2009) A novel small-subunit processome assembly intermediate that contains the U3 snoRNP, nucleolin, RRP5, and DBP4. *Molecular and cellular biology* **29**, 3007-3017
44. Pan, W. A., Tsai, H. Y., Wang, S. C., Hsiao, M., Wu, P. Y., and Tsai, M. D. (2015) The RNA recognition motif of NIFK is required for rRNA maturation during cell cycle progression. *RNA biology* **12**, 255-267
45. Champion, E. A., Lane, B. H., Jackrel, M. E., Regan, L., and Baserga, S. J. (2008) A direct interaction between the Utp6 half-a-tetratricopeptide repeat domain and a specific peptide in Utp21 is essential for efficient pre-rRNA processing. *Molecular and cellular biology* **28**, 6547-6556
46. Tafforeau, L., Zorbas, C., Langhendries, J. L., Mullineux, S. T., Stamatopoulou, V., Mullier, R., Wacheul, L., and Lafontaine, D. L. (2013) The complexity of human ribosome biogenesis revealed by systematic nucleolar screening of Pre-rRNA processing factors. *Molecular cell* **51**, 539-551
47. Dinman, J. D. (2005) 5S rRNA: Structure and Function from Head to Toe. *International journal of biomedical science : IJBS* **1**, 2-7
48. Kiparisov, S., Petrov, A., Meskauskas, A., Sergiev, P. V., Dontsova, O. A., and Dinman, J. D. (2005) Structural and functional analysis of 5S rRNA in *Saccharomyces cerevisiae*. *Molecular genetics and genomics : MGG* **274**, 235-247
49. Pestov, D. G., Lapik, Y. R., and Lau, L. F. (2008) Assays for ribosomal RNA processing and ribosome assembly. *Current protocols in cell biology* **Chapter 22**, Unit 22 11
50. Guertin, D. A., and Sabatini, D. M. (2009) The pharmacology of mTOR inhibition. *Sci Signal* **2**, pe24
51. James, M. J., and Zomerdijk, J. C. (2004) Phosphatidylinositol 3-kinase and mTOR signaling pathways regulate RNA polymerase I transcription in response to IGF-1 and nutrients. *The Journal of biological chemistry* **279**, 8911-8918
52. Tsang, C. K., Liu, H., and Zheng, X. F. (2010) mTOR binds to the promoters of RNA polymerase I- and III-transcribed genes. *Cell Cycle* **9**, 953-957
53. Mayer, C., and Grummt, I. (2006) Ribosome biogenesis and cell growth: mTOR coordinates transcription by all three classes of nuclear RNA polymerases. *Oncogene* **25**, 6384-6391
54. Mayer, C., Zhao, J., Yuan, X., and Grummt, I. (2004) mTOR-dependent activation of the transcription factor TIF-IA links rRNA synthesis to nutrient availability. *Genes & development* **18**, 423-434
55. Thoreen, C. C., Chantranupong, L., Keys, H. R., Wang, T., Gray, N. S., and Sabatini, D. M. (2012) A unifying model for mTORC1-mediated regulation of mRNA translation. *Nature* **485**, 109-113
56. Hsieh, A. C., Liu, Y., Edlind, M. P., Ingolia, N. T., Janes, M. R., Sher, A., Shi, E. Y., Stumpf, C. R., Christensen, C., Bonham, M. J., Wang, S., Ren, P., Martin, M., Jessen, K., Feldman, M. E., Weissman, J. S., Shokat, K. M., Rommel, C., and Ruggero, D. (2012) The translational landscape of mTOR signalling steers cancer initiation and metastasis. *Nature* **485**, 55-61
57. Kim, D. H., Sarbassov, D. D., Ali, S. M., King, J. E., Latek, R. R., Erdjument-Bromage, H., Tempst, P., and Sabatini, D. M. (2002) mTOR interacts with raptor to form a nutrient-sensitive complex that signals to the cell growth machinery. *Cell* **110**, 163-175
58. Sarbassov, D. D., and Sabatini, D. M. (2005) Redox regulation of the nutrient-sensitive raptor-mTOR pathway and complex. *The Journal of biological chemistry* **280**, 39505-39509
59. Chasse, H., Boulben, S., Costache, V., Cormier, P., and Morales, J. (2017) Analysis of translation using polysome profiling. *Nucleic acids research* **45**, e15
60. Marks, M. S. (2001) Determination of molecular size by zonal sedimentation analysis on sucrose density gradients. *Current protocols in cell biology* **Chapter 5**, Unit 5 3

61. Wang, M., and Pestov, D. G. (2016) Quantitative Northern Blot Analysis of Mammalian rRNA Processing. *Methods Mol Biol* **1455**, 147-157
62. Bochner, B. R., and Ames, B. N. (1983) Sensitive fluorographic detection of 3H and 14C on chromatograms using methyl anthranilate as a scintillant. *Analytical biochemistry* **131**, 510-515

FOOTNOTES

This work was supported by funding provided by the Cancer Prevention & Research Institute of Texas (CPRIT) grants RP130276 and RP140408 and also the startup funding provided by Nazarbayev University (to D.D.S.).

The abbreviations used are: rRNA, ribosomal ribonucleic acid; 40S and 60S, 40 and 60 Svedberg ribosomal subunits; RPS, ribosomal proteins of small subunit; RPL, ribosomal proteins of large subunit, IPRib, intermediate pre-ribosome; CPRib, composed pre-ribosome.



<p>85S</p> <p>Composed</p> <p>Pre-ribosome</p> <p><u>CPRib</u></p>	<p>105S 115S 125S</p> <p>#3 #2 #1</p> <p>Intermediate</p> <p>Pre-ribosomes</p> <p><u>IPRib</u></p>
------------------------------------------------------------------------------------------------	---------------------------------------------------------------------------------------------------------------------------------------

Figure 1. Detection of the native pre-ribosomal CPRib and IPRib complexes. The soluble nuclear fraction was obtained from the human A549 cancer cells and analyzed by a linear (0%-50%) sucrose gradient fractionation. The resolved RNP complexes were detected by a continuous monitoring of RNA absorbance at 254 nM using Biocomp Station with a Triax Flow Cell. The resolved CPRib (85S) and IPRib (105S-125S) RNP particles are indicated. Fractions: 17 and 18 (CPRib – 85S), 25 and 26 (IPRib1 – 125S), 23 and 24 (IPRib2 – 115S), 21 and 22 (IPRib 3 – 105S).

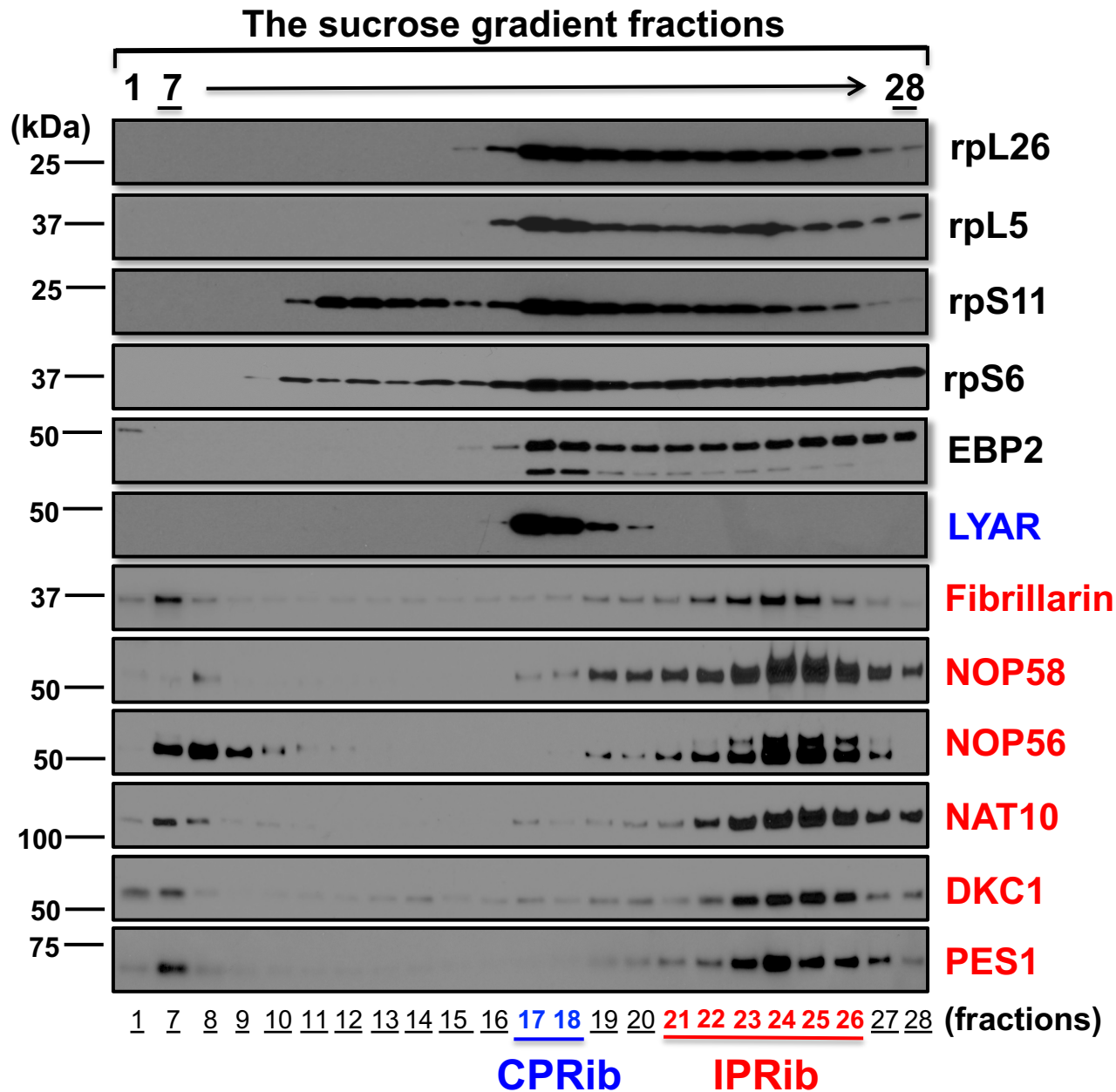


Figure 2. The CPRib and IPRib complexes are distinct pre-ribosomes that contain different ribosomal biogenesis factors. The soluble nuclear fraction obtained from A549 cancer cells were resolved by the sucrose fractionation and the fractions were analyzed by the immunoblotting with the indicated antibodies. The CPRib fractions and its component are shown in blue and the IPRib fractions and its components are shown in red.

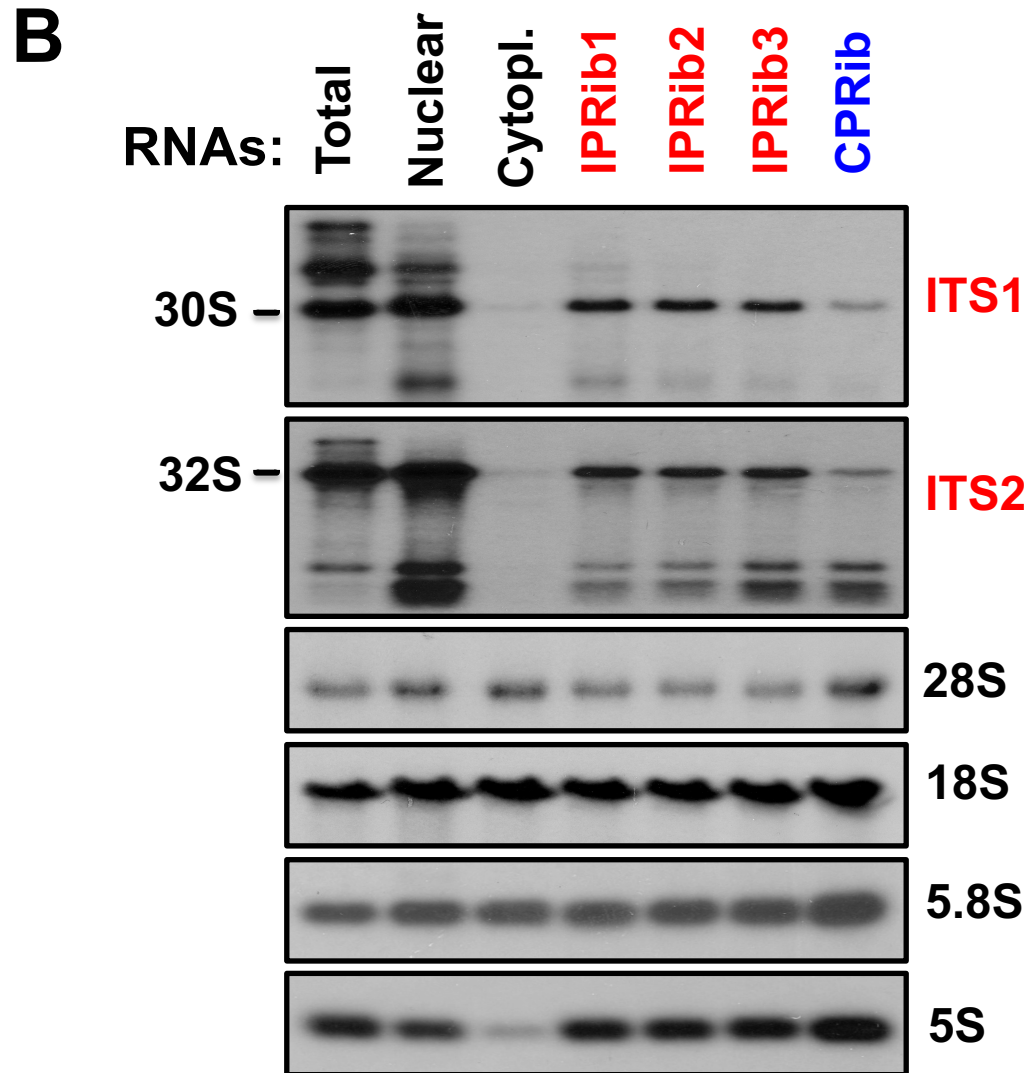
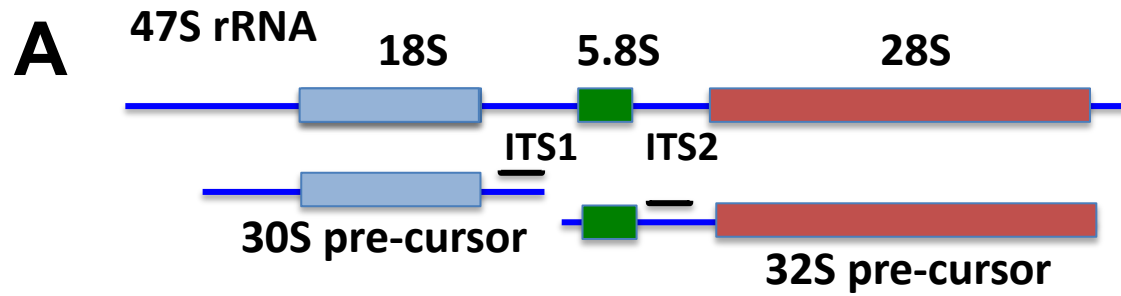


Figure 3. The 30S and 32S pre-cursor rRNAs are present in the nucleolar pre-ribosomal complexes but not in cytoplasm. **a** The schematic representation of the RNAs pre-cursors recognized by the ITS1 and ITS 2 probes. **b** The RNAs were isolated from IPRib and CPRib complexes and also total, nuclear and cytoplasmic fractions. A similar amount of RNA (5 microg) were resolved in agarose gel and analyzed by Northern blot analysis by probing the membrane with the indicated oligonucleotides complimentary to different areas of human 47S rRNA.

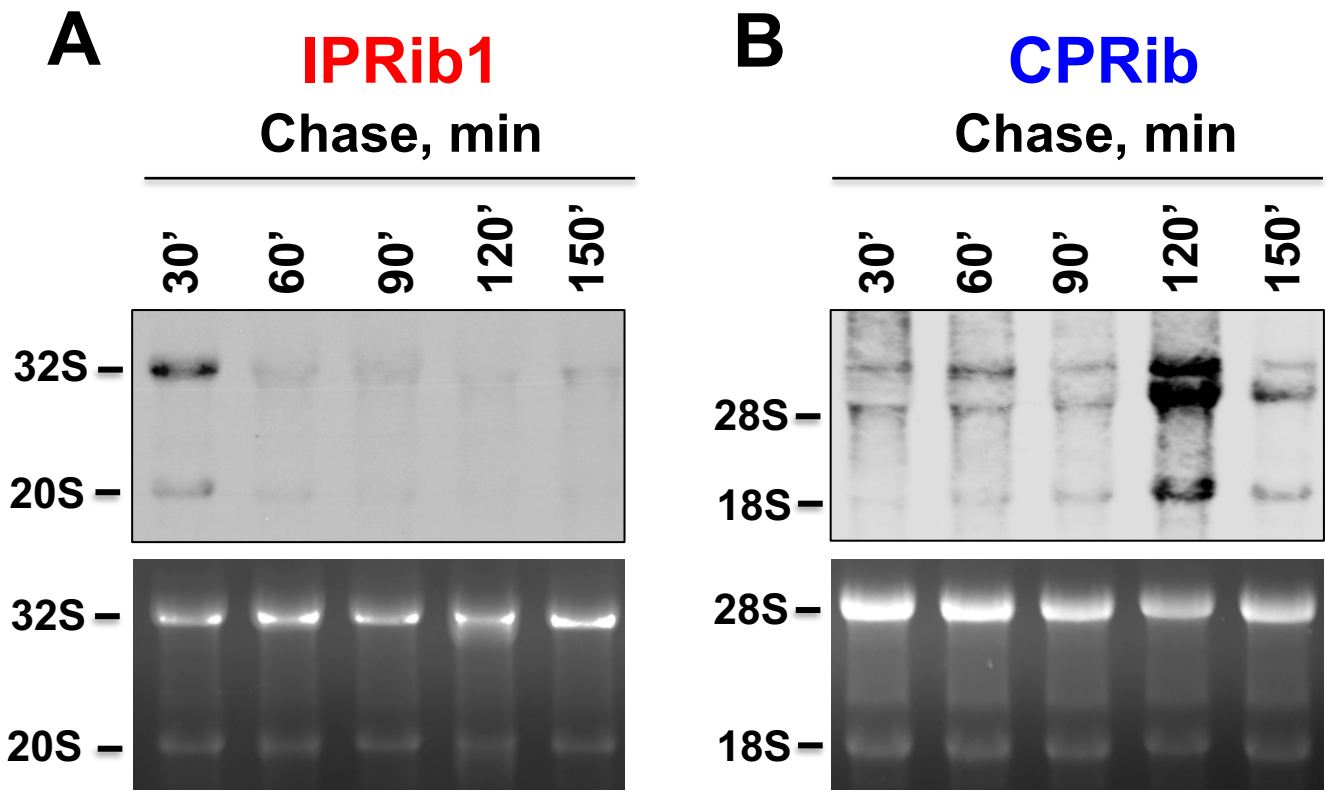


Figure 4. The IPRib assembly precedes formation of CPRib. The pulse-chase experiment was performed by [³H] uridine labeling of A549 cells for 30 min with the following replacement the cell culture medium containing non-labeled “cold” uridine for the indicated chase time. The nuclear fractions were resolved on sucrose gradient to obtain the pre-ribosomal complexes. The RNAs isolated from the fractions 25 and 26 representing IPRib1 (A) or the fractions 17 and 18 representing CPRib (B) complex were resolved on a gel and blotted to the membrane for the fluorographic detection of the [³H] labeled RNAs.

CURRENT: A549_control 1
OVERLAY: A549_-AA 1 hour

Calibration

Sample A.Zero: 779522.2
Source A.Zero: 257956.2

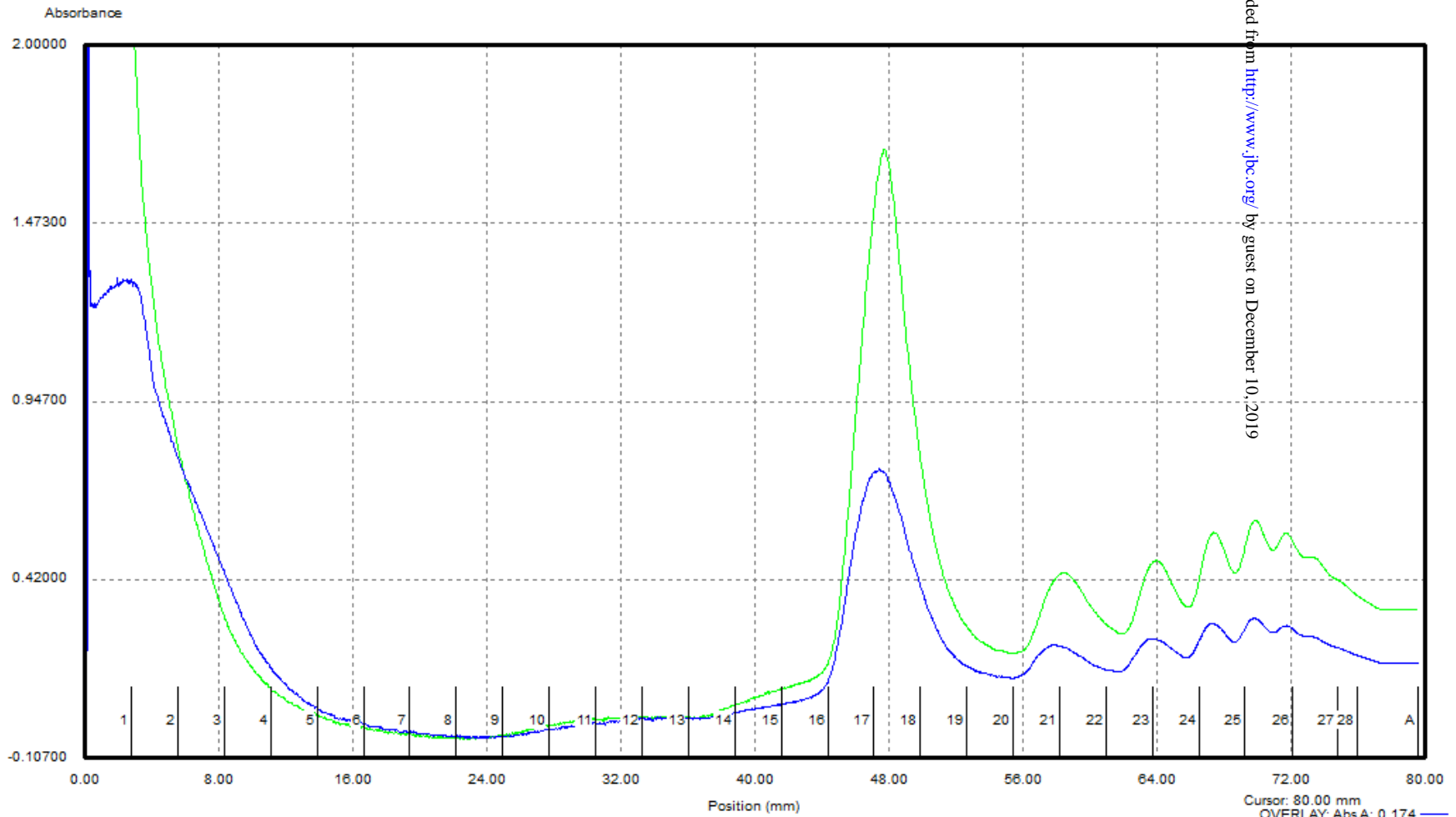


Figure 5. Abundance of re-ribosomal CPRib and IPRib complexes is sensitive to amino acid deprivation. A549 cells were incubated in the medium with or with amino acids (-AA) for one hour. The soluble nuclear fraction was obtained from cells and analyzed by a linear (0%-50%) sucrose gradient fractionation as described in Fig 1. The overlaying profiles of pre-ribosomal complexes are shown with control cells in green and amino acid (-AA) deprived cells for one hour in blue.

CURRENT: A549_control 1
OVERLAY: A549_-Torin 1 hour

Calibration

Sample A Zero: 779522
Source A Zero: 257956.2

Downloaded from <http://www.jbc.org/> by guest on December 10, 2019

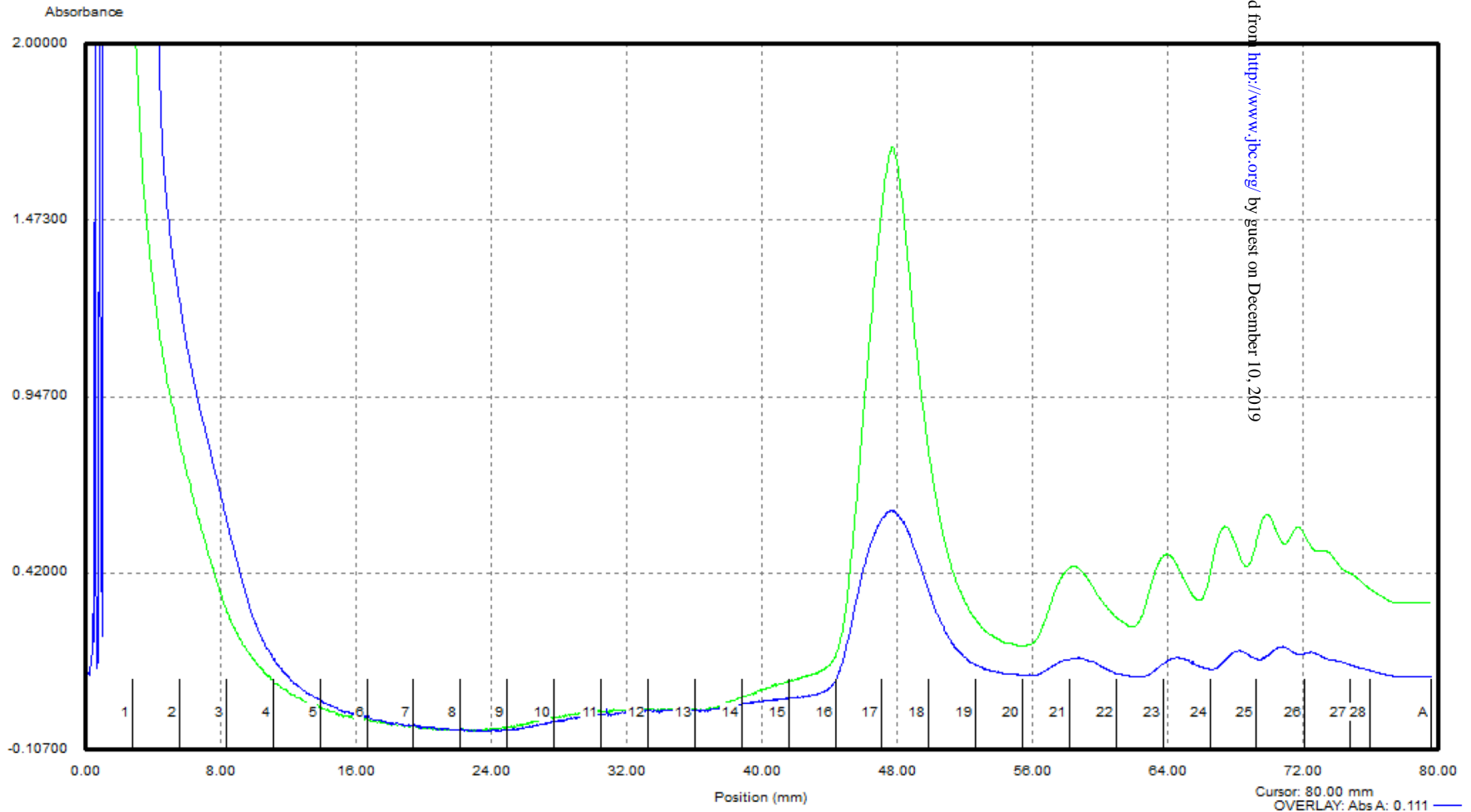


Figure 6. Abundance of re-ribosomal CPRib and IPRib complexes is sensitive to inhibition of the mTOR kinase activity. A549 cells were incubated with or without Torin 1 (250 nM) for one hour. The soluble nuclear fraction was obtained from cells and analyzed by a linear (0%-50%) sucrose gradient fractionation as described in Fig 1. The overlaying profiles of pre-ribosomal complexes are shown with control cells in green and Torin 1 treated cells for one hour in blue.

Formation of mammalian pre-ribosomes proceeds from intermediate to composed state during ribosome maturation

Danysh A. Abetov, Vladimir S. Kiyon, Assylbek A. Zhylkibayev, Dilara A. Sarbassova, Sanzhar D. Alybayev, Eric Spooner, Min Sup Song, Rakhmetkazhy I. Bersimbaev and Dos D. Sarbassov

J. Biol. Chem. published online May 10, 2019

Access the most updated version of this article at doi: [10.1074/jbc.AC119.008378](https://doi.org/10.1074/jbc.AC119.008378)

Alerts:

- [When this article is cited](#)
- [When a correction for this article is posted](#)

[Click here](#) to choose from all of JBC's e-mail alerts